Water Channel Experiments of Dynamic Stall on Darrieus Wind Turbine Blades

G. Brochier,* P. Fraunié,† and C. Béguier‡
Institut de Mécanique et Statistique de la Turbulence (IMST), Marseilles, France
and
I. Paraschivoiu§
Ecole Polytechnique de Montréal, Québec, Canada

An experimental study of periodic vortex phenomena was performed on a model of a two straight-bladed Darrieus wind turbine under controlled-rotation conditions in the Institute de Méchanique et Statistique de la Turbulence (IMST) water channel. The study focused on the tip-speed ratios at which dynamic stall appears. Observations of this phenomenon were made using dye emission and the hydrogen bubbles and photographs, movies, and video recordings were made. Velocity measurements were obtained using the laser-doppler velocimeter and the components of velocity fluctuations were determined quantitatively.

Nomenclature

c = profile chord
n = spectral frequency
R = rotor radius
Re = rotor Reynolds number, $=2RU_\infty/v$
rms = root mean square
t = profile thickness
$\overline{U}$ = local time-mean velocity
$\tilde{U}$ = mean mass flow velocity
U_∞ = freestream velocity
u' = rms value of the streamwise fluctuating velocity
v' = rms value of the crosswise fluctuating velocity
X, Y = cartesian coordinates
X/R = distance downstream divided by rotor radius
Y/R = distance perpendicular to the incoming flow divided by rotor radius
α = angle of attack
α_{ss} = static stall angle of attack
λ = tip-speed ratio, $=\omega R/U_\infty$
ω = angular speed of wind turbine rotor
ν = kinematic viscosity

Introduction

THE Darrieus vertical-axis wind turbine with curved or straight blades is a fixed pitch device and operates in a complex unsteady flow environment. During one rotation, the velocity of the flow relative to the aerofoil, which (to the first order) consists of the vector sum of the blade and wind speeds, varies cyclically in both magnitude and direction. In reality, this velocity is modified by the presence of induced velocities, tip vortices, and shed vorticity from the wake of the blade traversing the forward half of the circular trajectory. Both the unsteady flow and the wake crossing have a significant role in the loading on the blades.

A major aspect of the unsteady aerodynamics of the Darrieus rotor is the effect of dynamic stall, which occurs during starting or stopping, at low tip-speed ratios or in sudden gusts. The dynamic-stall effects can be seen on power performance curves which exceed steady flow predictions for tip-speed ratios less than 4. These effects strongly influence the drive train design, generator sizing, and overall system design. According to their vortex structure, the wakes of the blades and the central column generate aeroelastic vibrations of the rotor for different operating conditions. Thus, the ability to predict dynamic stall becomes of crucial importance in optimizing Darrieus wind turbine device.

To date, there is no analytical model capable of predicting lift and drag in the separated flow region on the Darrieus rotor blades, and the dynamic stall characteristics are approximated by using the Gormont model.[1] This stall model was developed especially for thin airfoils ($t/c<12\%$) and is not applicable for deep stall ($\alpha>\alpha_{ss}+5$ deg) applications.

Several experimental works have been published which deal with tunnel measurements or field tests which obtained the forces acting on a blade through stall and in post-stall, quantitative data which describes the wake region, and qualitative data from flow visualization. The pressure distribution measurements, which were made on the DOE/Sandia 17-m machine using flush-mounted pressure transducers and the data at tip-speed ratios ($\lambda=3.1$, 2.9. and 2.6), show that dynamic stall occurs on the upwind half-cycle of the rotor.[2] Flow visualization tests were performed on the same wind turbine using chemical sublimation. At Texas Tech University, a straight-bladed rotor was built and operated in a water channel to validate the major features of the vortex model.[3] In this case, the instantaneous-normal and tangential blade forces were measured as well as the velocity profiles in the rotor wake. The velocity profiles were measured using a hot-wire anemometer system.

At Sherbrooke University, several tests on a straight-bladed Darrieus rotor with a NACA 0018 blade section were conducted to determine aerodynamic forces or rotor performance in wind tunnel conditions,[4] and a validation of the loads predictions is given in Ref. 5. In Ref. 6, the effects of dynamic stall, as determined on an analog system of the real vertical-axis wind rotor are discussed. These effects were studied using pressure distribution and the smoke-wire flow visualization technique. The object of this work was to determine the flow characteristics inside and in the wake of a straight-bladed Darrieus rotor when operating in the dynamic stall mode.

Received Aug. 13, 1985; revision received Feb. 2, 1986.

*Graduate Student, Department of Mechanical Engineering.
†Research Scientist, Department of Mechanical Engineering.
‡Senior Scientist, Department of Mechanical Engineering.
§Associated Professor, Department of Mechanical Engineering. Member AIAA.

Models and Experimental Techniques

A major contribution with regard to experimental work was to obtain qualitative data from flow visualization and quantitative data from the measurements of velocity profiles through the rotor and in the wake using laser-doppler velocimetry (LDV).

The flow visualization in a water channel was effected by dye emission and by hydrogen-bubble techniques. The data in the form of the velocity profiles taken in the wake region at several streamwise locations behind the rotor were obtained by the LDV technique.

The LDV technique has several advantages with respect to other experimental methods, such as pitot tube or hot-wire, due to its nonintrusive probe, good spatial resolution, and high frequency response in water. The LDV is used by rear diffusion with the advantage of the forward diffusion. Other merits of the laser-doppler velocimeter are its linear response to velocity and capability for measuring one velocity component independently of the others in the fringe plane.

The water channel is vertical and works in continuous mode by gravity at constant level. The channel has a working section of 20×20 cm and a height of 1.5 m. The walls of the water channel were built of plexiglass, and this allowed the flow visualizations and LDV measurements at the same conditions to be done (simultaneously). The rotor is driven by a variable dc motor with field excitation controlled by a rheostat giving rotational speed variations up to 1000 rpm, which means that the entire operating range of the wind turbine is covered. Tip-speed ratios varying from 1 to 8 were explored for a rotor Reynolds number $Re = 10^4$. The experimental model characteristics are 1) blade profile, NACA 0018; 2) profile chord, 2 cm; 3) blade length, 20 cm; 4) rotation speed, variable from 100 to 1000 rpm; 5) rotor diameter, 2 R, 12 cm; and 6) central-column diameter, 1 cm.

The flow speed in the water channel was $U_\infty = 15$ cm/s. The central section of each blade is equipped with a dye injection part. The dye circuits feeding the two blades are independent, to enable us to distinguish between the wakes of the two blades. The central column has its own dye circuit which is connected to one of the blade dye circuits. Micropipettes are installed on the upwind side for observing the potential flow.

The complete system is located downstream from the nozzle of the Institut de Méchanique et Statistique de la Turbulence (IMST) water channel, so that when the aerofoil is at its maximum forward position it is 10 chord lengths downstream from the nozzle plane. Speed measurement is obtained form a photoelectric cell with a digital readout.

The aerofoil of 2 cm chord length was made of epoxy. Each blade has been obtained by molding, with the half part of the wheel disk used for the attachment to the axis of rotation. This experimental model will be able to work without the central tower. In this case, it is possible to use a laser mirror placed normal to the rotation axis to measure the velocities inside the rotor as can be seen in Fig. 1.

The span of the complete aerofoil is 20 cm, and the surface was polished smooth to avoid any slight mismatch at the joints between the sections. End plates were also added to prevent any significant induced flows arising from end effects, so an infinite aspect-ratio flow as obtained near the center line (the geometric aspect-ratio was equal to 10). The experimental model represents a rigid structure that was capable of sustaining a constant centrifugal force. There were no significant vibrations or instability detected.

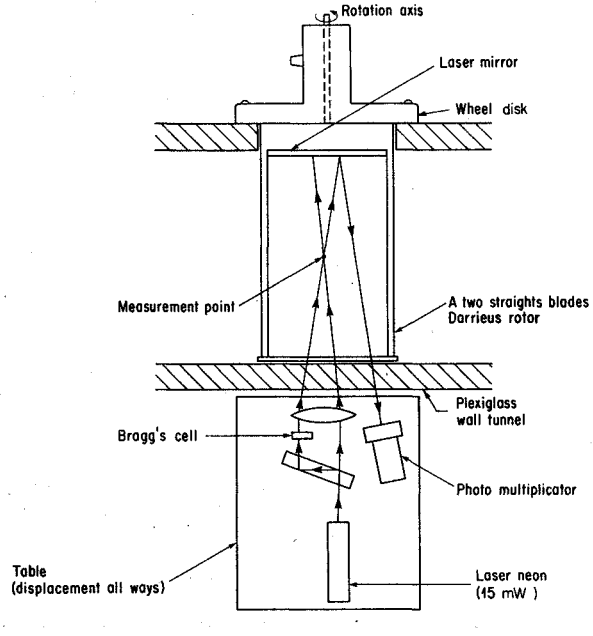

Fig. 1 Experimental geometry of the LDV system.

Results and Discussion

During the rotation of a blade, its incidence varies in magnitude and also changes sign. This results in successive separation and reattachment of the boundary layer on the profile. Small λ dynamic stall causes an increase in the lift following the blade stall only for large α_{ss}.

In Fig. 2, the evolution of the longitudinal mean velocities ratios $U/\tilde{U}$, where $\tilde{U}$ is the mean mass flow velocity, is presented. The different measured profiles have been obtained in the wake of the rotor, and one profile shows the upstream velocities ($X/R = -1.67$). The slight velocity gradient characterizes the upstream increment of the flow due to the rotational effect of the blade. The measurements are presented for $\lambda = 2.14$ in Fig. 2 and $\lambda = 3.85$ in Fig. 3. The latter value ($\lambda = 3.85$) corresponds to an operating regime without dynamic stall and the former value with dynamic-stall effects. For the two cases, a slight asymmetry in the mean velocity profiles giving a displacement of the minimum velocity from the median plane of the channel can be noted.

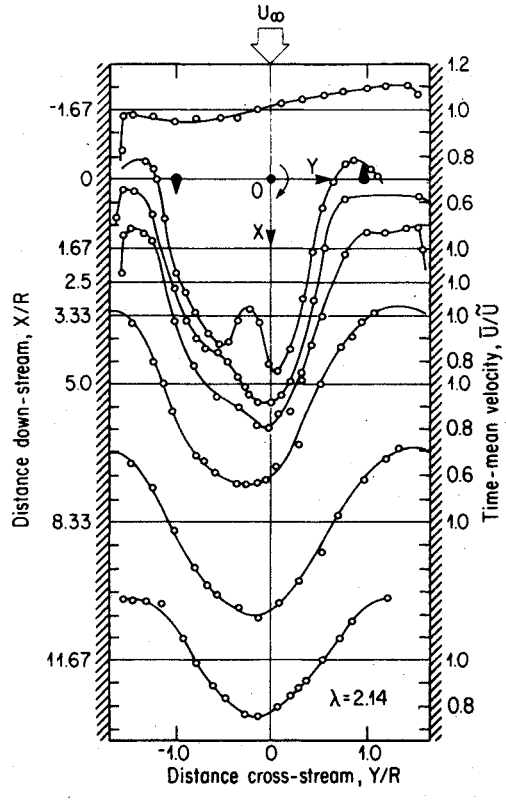

Fig. 2 Streamwise mean velocity profiles for $\lambda = 2.14$.

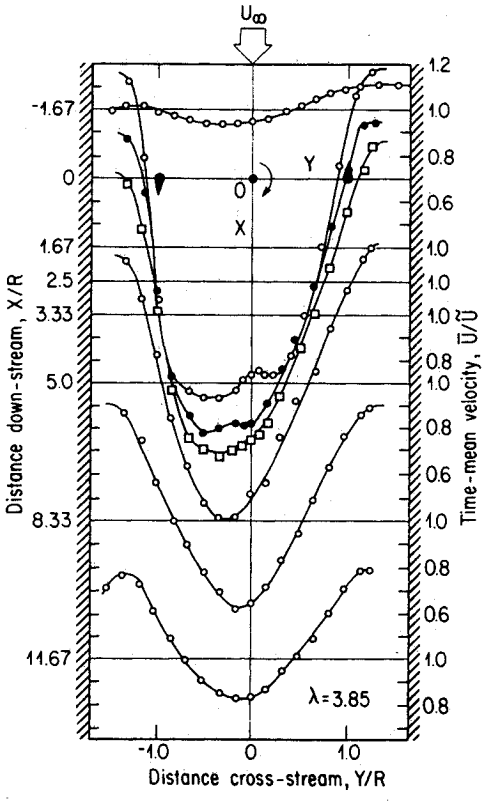

Fig. 3 Streamwise mean velocity profiles for $\lambda = 3.85$.

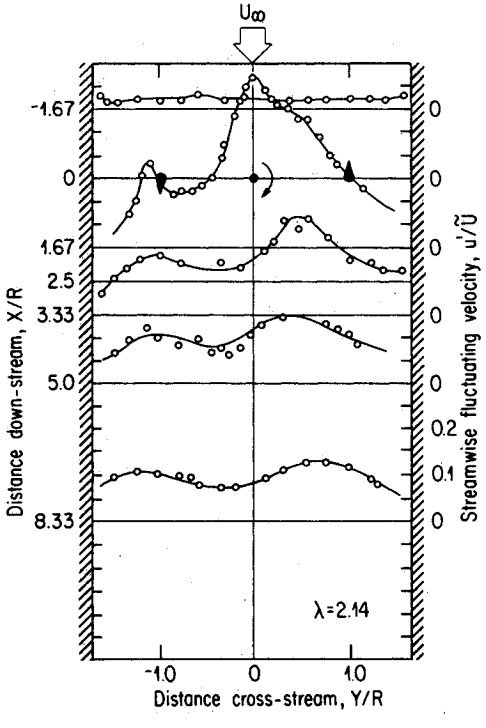

Fig. 4 Streamwise fluctuating velocity for $\lambda = 2.14$.

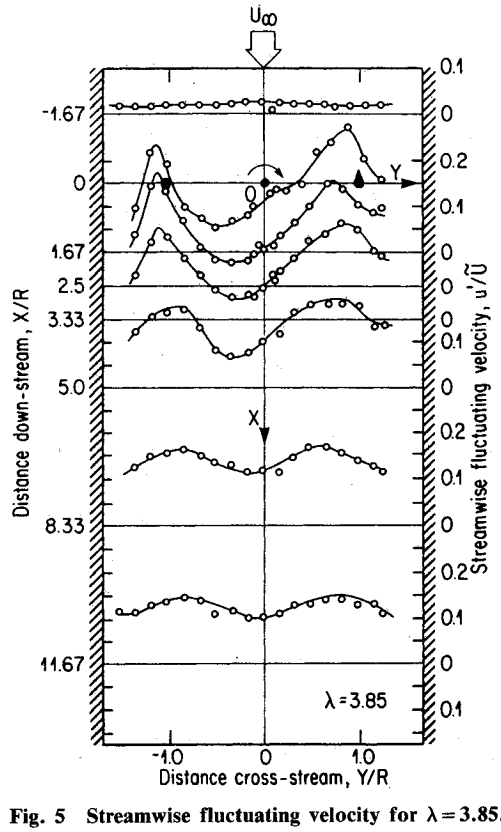

Fig. 5 Streamwise fluctuating velocity for $\lambda = 3.85$.

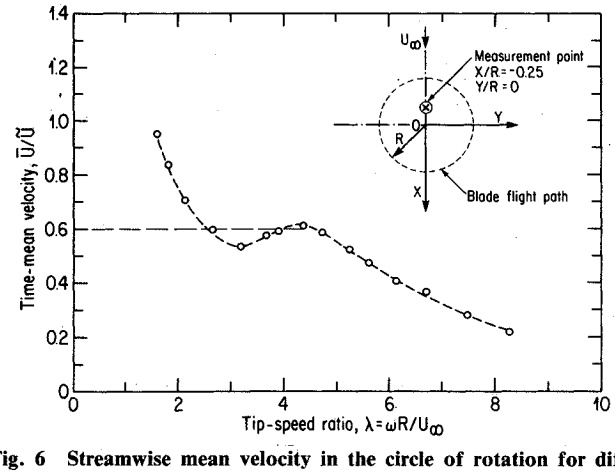

Fig. 6 Streamwise mean velocity in the circle of rotation for different λ values at $X/R = 0.25$ and $Y/R = 0$.

However, the most significant effect appearing in the velocity profile distribution is the "inverse wake effect" which can be seen in the downstream locations up to X/R of about 5 (Figs. 2 and 3).

The turbulence intensity profiles for the two studied cases are shown in Figs. 4 and 5. They tend toward two-maxima almost-symmetrical wake profile. However, a difference between the two maxima appears in the near wake: the higher one being on the side where the velocities of the blade and the flow velocity have the same sign. This fact is due to the generation on this side of stall vortices which have been put in evidence by the visualization techniques described above.

Measurements of the longitudinal mean velocity ratio $\bar{U}/\tilde{U}$ inside the circle of rotation are presented in Fig. 6. These measurements have been obtained at a point at $X/R = -0.25$ and $Y/R = 0$; i.e., in front of the central tower. A mirror installed at the rotor base served for velocity measurements inside the circle of rotation. The results show a decreasing of the velocity ratio with increasing of the tip-speed ratio λ up to a plateau in the range $5 > \lambda > 3$ corresponding to the normal working conditions of the rotor. This plateau occurs for a value about $\bar{U}/\tilde{U} = 0.6$, corresponding rather well to the theoretical value obtained with a two actuator-disks model.[7]

Figure 7 illustrates the fluctuating velocity components (in the y direction) at different locations inside the circle of rota-

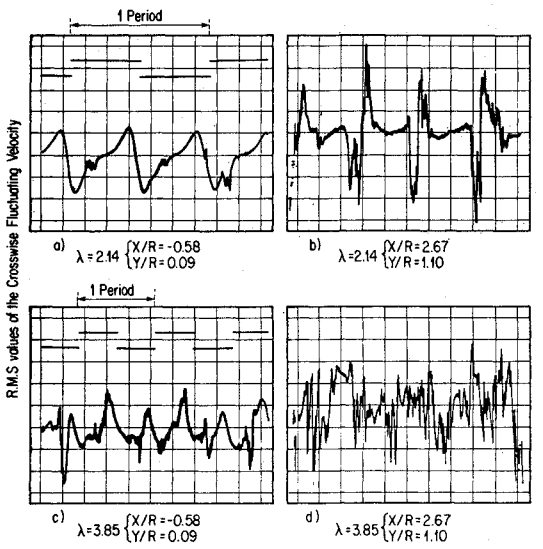

Fig. 7 Oscillograms of the crosswise fluctuating velocity

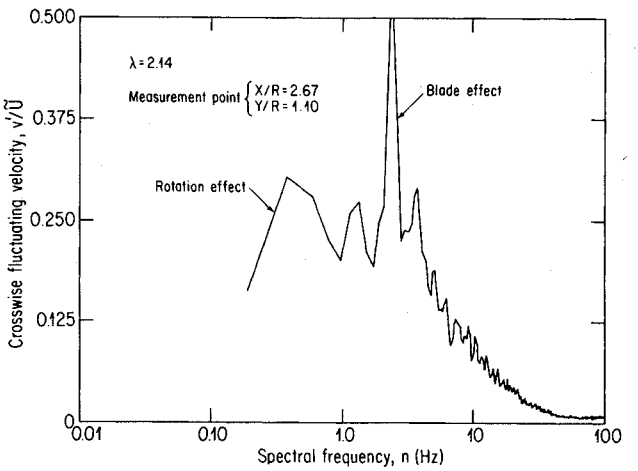

Fig. 8 Crosswise fluctuating velocity vs spectral frequency for $\lambda = 2.14$.

tion, $X/R = 0.58$ and $Y/R = 0.09$ (Figs. 7a and 7c); and in the wake flow, $X/R = 2.67$ and $Y/R = 1.10$ (Figs. 7b and 7d). These two points have been selected from the visualizations. They correspond to the passage of vortices created during the dynamic stall. These oscillograms show the fluctuation velocity due to the passage of the blade wakes, which is rather periodic in the case $\lambda = 2.14$ (Figs. 7a and 7b) but less stable in the case $\lambda = 3.85$ (Figs. 7c and 7d). The loop signals at the top of Figs. 7a and 7c represent the passage of the blades detected by a photoelectric cell. The spectrum of this signal (Fig. 7b) is plotted in Fig. 8. It shows a high peak for the periodic contribution of the blades but also a significant effect at the rotation frequency which represents approximately half of the blades effect.

The use of the water as a working fluid facilitated the ability to visualize the flow structure while operating at appropriate blade Reynolds numbers. Finally, in Figs. 9 and 10, two results obtained by the visualization technique for the dynamic stall case of $\lambda = 2.14$ are presented. This case corresponds to the formation of a contrarotating vortices doublet in the right part of the blade trajectory as shown in Fig. 9. In the $\lambda = 2.14$ case, this vortices doublet, corresponding to the emission of a leading edge vortex followed by a trailing edge one, goes on the blade trajectory. It can be related to the overlift that has been measured during the dynamic stall. Different positions of this doublet during the

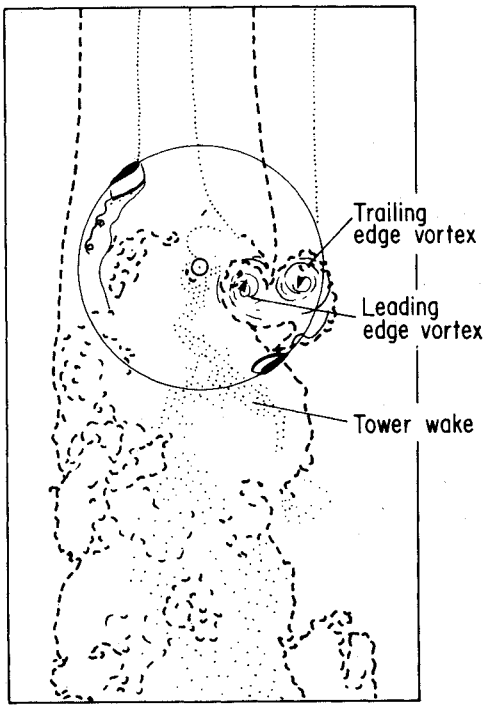

Fig. 9 Flow visualization in the dynamic stall condition for $\lambda = 2.14$.

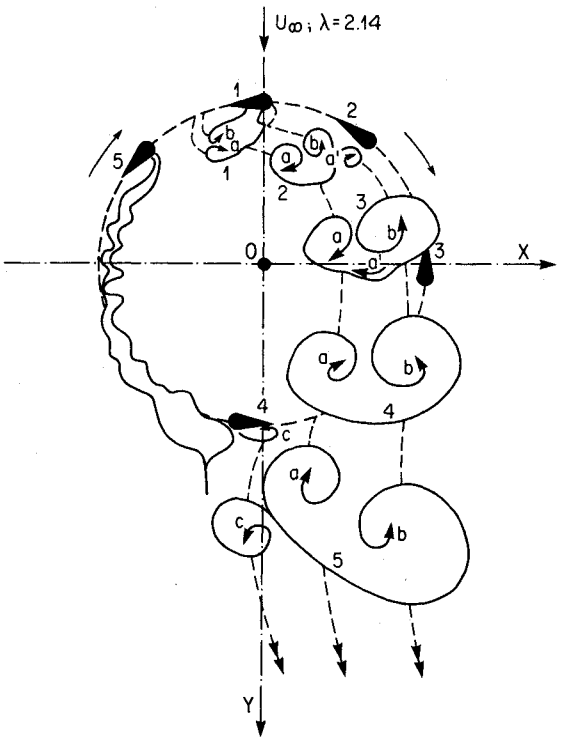

Fig. 10 Schematic diagram of the vortex shedding for $\lambda = 2.14$.

rotation have been drawn in Fig. 10. This figure shows the doublet from its emission up to its diffusion in the wake. This doublet is followed by another weaker one, emitted in the downstream part of the blade trajectory. In the going upstream of the blade trajectory (left part of trajectory), only a slight incidence wake is created because the blade airfoils encounter smaller angles of attack. Thus, it is clear that in the dynamic stall condition, an asymmetry, between the left and the right sides of the rotation circle exists, in addition to the upstream and downstream asymmetry, which is

generally considered in the double disks model.[5] The results presented in Figs. 9 and 10, when the rotor was driven by a motor, are similar to those obtained when the rotor was driven by the fluid at the same turbulence level flow and for a given rotation speed. This can be explained by the similarity of the induced velocities variation vs blade position at low tip-speed ratios (in the dynamic stall condition).

The test conditions of these experiments represent a two-dimensional low turbulence level flow while the measurements in the site conditions[2] are made in a three-dimensional high turbulence level atmospheric flow. It is known that in the low turbulence conditions the dynamic-stall effects are more significant with respect to high turbulence level.[6,8] In the two-dimensional study, the spanwise velocity effect on the blade, which can influence the dynamic stall behavior, was not considered.

Conclusion

The results show that dynamic stall causes rather unsual vortex shedding that appears in the form of two counter-rotating vortices on the right part of the circle of rotation (at the point where the blade velocity and the flow velocity are in the same direction). The first vortex is shed at the leading edge of the blade and turns in the same direction as the rotor; whereas, the second vortex shedding occurs at the trailing edge and turns in the opposite direction. This vortex system is convected by the mean flow through the inside. In the case of a tip-speed ratio $\lambda = 2.14$, this doublet crosses the blade in midpath and contributes to an increase in the lift. This phenomenon has already been observed on experimental Darrieus wind turbines, such as the Sandia National Laboratories' and Magdlen Island's machines.

The phenomena described were also observed in a spectral study of the components of velocity fluctuations which were determined quantitatively. The variations in the mean wake show a number of additional features compared to a typical wake of a plane obstacle. For the Darrieus rotor, a blade in the downstream location passes through the wake flow (of reduced momentum flux) shed by the blade when in the upstream locations.

In addition, the locations of blade/wake interactions have been identified. These interactions multiply at higher tip-speed ratios (where dynamic-stall vortices no longer appear) and the entire flow inside the rotor is progressively perturbed.

Characterization and understanding of dynamic-stall phenomena are indispensible for modeling the flow and calculating the cyclic areodynamic forces to be taken into consideration. Thus, recent work[8] shows good improvement to the aerodynamic-performance prediction by applying Gormont's dynamic-stall model according to flow visualization asymmetry of current work.

Acknowledgment

This investigation has been supported financially in part by NSERC Grant A-4556, and by Coopération France-Québec.

References

[1]Gormont, R. E., "A Mathematical Model of Unsteady Aerodynamics and Radial Flow for Application to Helicopter Rotors," U.S. Army Air Mobility R&D Laboratory, Vertol Division, Philadelphia, PA, Rept. on Boeing-Vertol Contract DAAJ02- 71-C-0045, May 1973.

[2]Akins, R. E., Klimas, P. C., and Croll, R. H., "Pressure Distributions on an Operating Vertical Axis Wind Turbine Blade Element," *Proceedings of the American Solar Energy Society Annual Meeting, Sixth Biennial Wind Energy Conference,* Minneapolis, MN, June 1983, pp. 455-462.

[3]Strickland, J. H., Smith, T., and Sun, K., "A Vortex Model of the Darrieus Turbine: An Analytical and Experimental Study," Sandia National Laboratories, Albuquerque, NM, SAND 81-7017, June 1981.

[4]Vittecoq, P. and Laneville, A., "Etude en soufflerie d'un rotor de type Darrieus," Mechanical Engineering Department, University of Sherbrooke, Québec, Canada, Rept. MEC-82-2, Aug. 1982. (report submitted to Institut de Recherche d'Hydro-Québec).

[5]Paraschivoiu, I., "Predicted and Experimental Aerodynamic Forces on the Darrieus Rotor," *Journal of Energy,* Vol. 7, Nov.-Dec., 1983, pp. 610-615.

[6]Vittecoq, P. and Laneville, A., "Etude expérimentale du décrochage dynamique dans le cas du rotor Darrieus," Mechanical Engineering Department, University of Sherbrooke, Québec, Canada, Rept. MEC-84-6, Dec. 1984 (report submitted to Institut de Recherche d'Hydro-Québec).

[7]Brochier, G., "Etude numérique de la couche limite instationnaire sur un profil d'aile en mouvement, application et expérimentation á l'éolienne Darrieus," Ph.D. Thesis, Université d'Aix Marseille II, Marseille, France, March 1986.

[8]Paraschivoiu, I., "Some Refinements to the Aerodynamic-Performance Prediction for Vertical-Axis Wind Turbines," Presented to the 5th Aerodynamic Seminar on Darrieus Turbine, Sandia National Laboratories, Albuquerque, NM, Jan. 1986.